Journal of the Optical Society of America B
OPTICAL PHYSICS

Optimizing the time resolution of supercontinuum spectral interferometry

J. K. Wahlstrand,* S. Zahedpour, and H. M. Milchberg

Institute for Research in Electronics and Applied Physics, University of Maryland, College Park, Maryland 20742, USA
**Corresponding author: wahlstrj@umd.edu*

Received 7 March 2016; revised 19 May 2016; accepted 1 June 2016; posted 1 June 2016 (Doc. ID 260564); published 20 June 2016

Single-shot supercontinuum spectral interferometry is a powerful technique for measuring transient refractive index changes. In principle, its time resolution is limited only by the available probe bandwidth. However, this assumes that the phase extraction has sufficient spectral resolution and that the probe spectral phase is exactly known. Using an analytical model for the spectral phase and amplitude modulation of a chirped probe pulse by a weak transient phase perturbation, we show how the probe chirp and spectral resolution determine the achievable time resolution. A simple, practical technique for precise *in situ* measurement of the probe spectral phase is described in detail, and the sensitivity of the extracted temporal phase profile to uncertainty in the probe spectral phase is demonstrated in numerical simulations.

OCIS codes: (120.3180) Interferometry; (320.7100) Ultrafast measurements.

http://dx.doi.org/10.1364/JOSAB.33.001476

1. INTRODUCTION

Single-shot supercontinuum spectral interferometry (SSSI) is used to measure the time- and space-dependent refractive index shift induced in a medium by an intense pump pulse [1]. In this method, two replica chirped supercontinuum (SC) pulses—one a reference pulse that precedes the pump pulse through the medium and the other a probe pulse that temporally overlaps the pump—interfere in the spectral domain, as viewed in the image plane of an imaging spectrometer. Fourier transform analysis of the resulting spectral interferogram enables extraction of the pump-induced transient phase shift imposed on the probe and, thus, the time-dependent refractive index shift. The ultimate time resolution is approximately the inverse of the bandwidth of the SC [1]. The SC pulse is typically generated by filamentation of ultrashort 800 nm pulses in a high-pressure Xe or SF_6 cell [2–5], and its broad bandwidth (typically >150 nm) enables a time resolution better than 10 fs. The ability to resolve, on this time scale, ultrafast refractive index transients induced by intense pump pulses was crucial for recent measurements of the optical nonlinearity near the ionization threshold [2,3], for cleanly distinguishing the electronic and inertial nonlinear responses in the molecular gases N_2, O_2, H_2, and D_2 [4–6], and the first direct measurements, for pump pulses in the mid-infrared, of the nonlinear refractive index of gas phase atoms and molecules [7]. Other important laser-driven dynamics, such as field ionization, can occur over even shorter time scales, which raises the question of how close to the ultimate theoretical time resolution is attainable by SSSI.

In this paper, we show that pushing SSSI to its ultimate time resolution requires extraction of the probe pulse's frequency domain phase and amplitude with a spectral resolution that depends on the magnitude of the probe chirp. It also requires precise knowledge of the probe spectral phase. In this paper, we also develop a simple, practical technique for *in situ* measurement of the probe spectral phase, and the sensitivity of the extracted transient phase shift to the probe spectral phase is demonstrated analytically and with numerical simulations.

In most of our previous experiments using SSSI, the SC spectral phase was determined only through the second order (the group delay dispersion or GDD) by examining the frequency dependence of the spectral phase shift on the pump–probe time delay [1], which is described in the following. This was sufficient for the time resolution required in those experiments [2–5], where the fastest dynamics followed the laser pulse envelope of FWHM $> \sim 40$ fs. However, higher-order corrections to the spectral phase improve the time resolution of SSSI and enable measurements of even faster transients. Here, we show that easily measured changes in the probe spectrum versus pump–probe delay can be used to measure the SC spectral phase to arbitrary order. We demonstrate the effect on the achievable time resolution of including successive orders of spectral dispersion in the analysis.

2. BACKGROUND

We first describe SSSI in detail. A strong pump pulse propagating along z in a medium induces a time- and

space-dependent change in the refractive index $\Delta n(x, y, z, t)$, which imparts a time-dependent phase shift,

$$\Delta\Phi(x, y, t) = k_0 \int \Delta n(x, y, z, t)\mathrm{d}z \approx k_0 L_{\mathrm{eff}} \Delta n(x, y, t),$$

on a co-propagating chirped probe pulse, where L_{eff} is the effective medium length and k_0 is the probe central wavenumber. Use of an imaging spectrometer enables 1D space-resolved transient measurements $\Delta\Phi(x, y_0, t)$ in a single shot, where x is aligned along the entrance slit and y_0 is the transverse location of the 1D x slice. Dropping the spatial dependence to simplify the notation, the probe field is given by

$$E_{\mathrm{pr}}(t) = \overline{E}_{\mathrm{pr}}(t) e^{i\Delta\Phi(t)}, \quad \textbf{(1)}$$

where E_{pr} ($\overline{E}_{\mathrm{pr}}$) is the probe field perturbed (unperturbed) by the pump pulse, and where $\Delta\Phi(t)$ is real. The fields E_{pr} and $\overline{E}_{\mathrm{pr}}$ are expressed in the frequency domain as $E_{\mathrm{pr}}(\omega) = |E_{\mathrm{pr}}(\omega)| e^{i[\phi_s(\omega)+\Delta\phi(\omega)]}$ and $\overline{E}_{\mathrm{pr}}(\omega) = |\overline{E}_{\mathrm{pr}}(\omega)| e^{i\phi_s(\omega)}$, where $E(\omega) = F\{E(t)\}$ is the Fourier transform of $E(t)$, $\phi_s(\omega)$ is the spectral phase of the unperturbed SC probe, and $\Delta\phi(\omega)$ is the change in spectral phase induced by the pump. Using Eq. (1), we find

$$\Delta\Phi(t) = \mathrm{Im}\left(\ln\left[\frac{F^{-1}\{|E_{\mathrm{pr}}(\omega)| e^{i\phi_s(\omega)+i\Delta\phi(\omega)}\}}{F^{-1}\{|\overline{E}_{\mathrm{pr}}(\omega)| e^{i\phi_s(\omega)}\}}\right]\right), \quad \textbf{(2)}$$

where F^{-1} denotes the inverse Fourier transform. Measurements of four quantities are required to reconstruct the time-domain phase shift: $|\overline{E}_{\mathrm{pr}}(\omega)|$, $\Delta\phi(\omega)$, $|E_{\mathrm{pr}}(\omega)|$, and $\phi_s(\omega)$. The first is simply the unperturbed probe spectral magnitude, which is easily found from the power spectrum $\overline{S}_{\mathrm{pr}}(\omega) \equiv |\overline{E}_{\mathrm{pr}}(\omega)|^2$. The next two are found from analysis of the spectral interferogram [1,8,9].

The fourth quantity is the unperturbed probe spectral phase $\phi_s(\omega)$. The probe pulse is chirped, mostly from dispersion in the optics after the SC generation cell. As previously mentioned, in previous work, $\phi_s(\omega)$ was found by examining the dependence of the frequency domain phase shift $\Delta\phi(\omega)$ on the pump–probe time delay in a nonlinear Kerr medium [1]. The best fit of peak phase shift frequency versus delay is linear, reflecting the leading quadratic term in the spectral phase, $\phi_s(\omega) = \beta_2(\omega - \omega_c)^2$, where ω_c is an arbitrarily defined central frequency, and β_2 was found from the fit [1].

Here, we apply the same pump–probe delay procedure to the differential probe power spectrum [10]:

$$\Delta S_{\mathrm{pr}}(\omega) \equiv |E_{\mathrm{pr}}(\omega)|^2 - |\overline{E}_{\mathrm{pr}}(\omega)|^2,$$

which is a more easily measured quantity. We also show that, for a sufficiently chirped probe pulse, we can measure higher-order corrections to $\phi_s(\omega)$, making better SSSI time resolution possible.

3. ANALYTICAL MODEL FOR SPECTRAL PHASE AND AMPLITUDE PERTURBATION

The phase perturbation $\Delta\Phi(t)$ imparted on the probe by the pump-induced refractive index change depends on the nature of the nonlinearity, which can be a combination of a nearly instantaneous electronic response as in the noble gases, a delayed inertial response from rotations or vibrations in molecular gases or condensed matter, or a cumulative nonlinearity from, for example, ionization. For peak phase perturbations satisfying $|\Delta\Phi(t)|_{\mathrm{max}} \ll 1$, (which we can ensure experimentally by keeping L_{eff} small), $e^{i\Delta\Phi(t)} \approx 1 + i\Delta\Phi(t)$, so Eq. (1) becomes $E_{\mathrm{pr}}(t) = \overline{E}_{\mathrm{pr}}(t) + i\Delta\Phi(t)\overline{E}_{\mathrm{pr}}(t)$. Taking the Fourier transform gives

$$E_{\mathrm{pr}}(\omega) = \overline{E}_{\mathrm{pr}}(\omega) + \frac{i}{2\pi}\int_{-\infty}^{\infty} \Delta\Phi(\omega - \omega')\overline{E}_{\mathrm{pr}}(\omega')\mathrm{d}\omega', \quad \textbf{(3)}$$

where the spectral phase,

$$\phi_s(\omega) = \beta_2(\omega_c)(\omega - \omega_c)^2 + \beta_3(\omega_c)(\omega - \omega_c)^3 + \ldots, \quad \textbf{(4)}$$

is implicit to $\overline{E}_{\mathrm{pr}}(\omega)$ and where the constant and linear phase terms giving the absolute phase and time delay are neglected.

Example simulations, using Eq. (3), of the probe power spectrum $|E_{\mathrm{pr}}(\omega)|^2$ in a medium with an instantaneous (electronic) nonlinearity are shown in Fig. 1. The probe's nonlinear phase shift is $\Delta\Phi(t) = 4\pi n_2 I(t) L_{\mathrm{eff}}/\lambda$, where $I(t)$ is the pump intensity peaking at 8×10^{13} W/cm^2, λ is the probe wavelength, and where we use $n_2 = 10^{-19}$ cm^2/W for the Kerr coefficient and $L_{\mathrm{eff}} = 0.4$ mm for the effective interaction length, all typical parameters in our experiments [3]. The pump pulse is taken to be a 60 fs FWHM Gaussian, and the SC probe amplitude $|\overline{E}_{\mathrm{pr}}(\omega)|$ is a Gaussian centered at 550 nm with 100 nm FWHM. This spectral width is easily achieved experimentally by filamentation in an Xe gas cell. Figure 1(a) shows

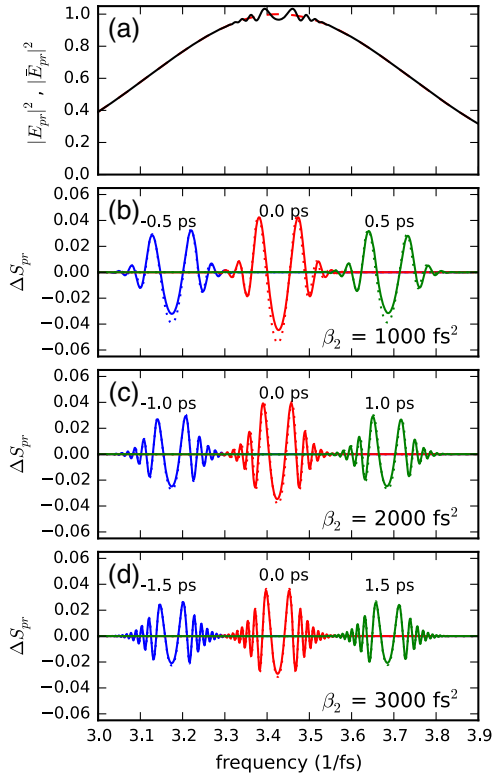

Fig. 1. Numerical simulation of the effect of a short pulse on the probe spectrum. (a) Normalized probe power spectrum with (solid black) and without (dashed red) a 60 fs pump pulse. (b)–(d) Numerically calculated differential probe spectrum $\Delta S_{\mathrm{pr}}(\omega)$ (solid) and the approximate expression [Eq. (5)] (dotted) for three values of β_2 and three pump–probe time delays.

the probe spectrum with and without the pump pulse. Figures 1(b), 1(c), and 1(d) show the differential probe spectrum $\Delta S_{\mathrm{pr}}(\omega)$ for $\beta_2 = 1000$, 2000, and 3000 fs^2, respectively, and $\beta_n = 0$ for $n > 2$. Plots are shown for three pump–probe time delays.

In order to understand the origin of the pump-induced oscillations in $\Delta S_{\mathrm{pr}}(\omega)$ and explicitly show how the probe spectral phase is extracted, we approximate the convolution integral of Eq. (3) using the method of stationary phase. To do so, we first note that $\Delta\Phi(\omega) = \Delta\Phi_0(\omega)e^{i\omega\tau_p}$ for a pump pulse at time delay τ_p, where $\Delta\Phi_0(\omega)$ is $F\{\Delta\Phi(t)\}$ at zero pump delay, so that the integrand's rapidly varying phase is $\phi(\omega') = \phi_s(\omega') + (\omega - \omega')\tau_p$. The integrand strongly oscillates in ω except near ω_0, where $\phi'(\omega' = \omega_0) = 0$, or $\phi_s'(\omega_0) = \tau_p$, so that the dominant contribution to the integral in Eq. (3) occurs near ω_0, yielding

$$E_{\mathrm{pr}}(\omega) \approx \overline{E}_{\mathrm{pr}}(\omega) - (i/2\pi)\Delta\Phi(\omega - \omega_0)\overline{E}_{\mathrm{pr}}(\omega_0)e^{i\pi/4}[\pi/|\beta_2(\omega_0)|]^{1/2},$$

an expression that is most accurate over bandwidths $|\omega - \omega_0| > \sim|1/\beta_2|^{1/2}$, or for large chirps. To the lowest-order in $\Delta\Phi$, the change in the probe power spectrum is, therefore,

$$\Delta S_{\mathrm{pr}}(\omega) \approx -|\Delta\Phi(\omega - \omega_0)\overline{E}_{\mathrm{pr}}(\omega_0)\overline{E}_{\mathrm{pr}}(\omega)|(\pi|\beta_2(\omega_0)|)^{-1/2} \times \cos(\phi_s(\omega) - \phi_s(\omega_0) + (\omega_0 - \omega)\tau_p + \pi/4). \quad (5)$$

The pump-induced change in the probe spectral phase is

$$\Delta\phi(\omega) \approx \Delta\Phi(\omega - \omega_0)\left[\frac{\pi}{|\beta_2(\omega_0)|}\right]\frac{\overline{E}_{\mathrm{pr}}(\omega_0)}{\overline{E}_{\mathrm{pr}}(\omega)} \times \cos(\phi_s(\omega) - \phi_s(\omega_0) + (\omega - \omega_0)\tau_p - \pi/4). \quad (6)$$

The accuracy of Eq. (5) is assessed in Figs. 1(b)–1(d), where its curves (dotted lines) are compared with numerical simulations of $\Delta S_{\mathrm{pr}}(\omega)$ (solid lines). As expected, the approximation works best for large β_2, but, in all cases, it reproduces the general shape of $\Delta S_{\mathrm{pr}}(\omega)$, in particular the location of the central minimum at $\omega = \omega_0$. Comparison of simulations of $\Delta\phi(\omega)$ with the approximation of Eq. (6), shown in Fig. 2, shows a similar level of accuracy.

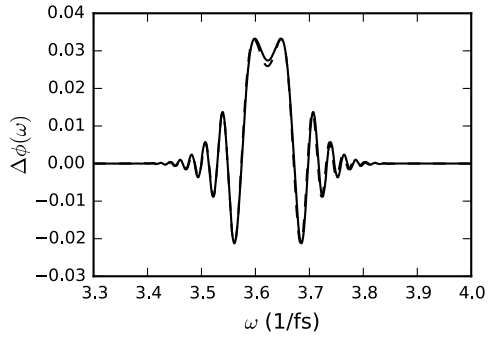

Fig. 2. Numerical simulation of pump-induced change in the probe spectral phase and comparison to Eq. (6), for the same parameters as used in Fig. 1, for $\beta_2 = 1000$ fs^2.

4. MEASURING THE PROBE SPECTRAL PHASE

Our technique for precise measurement of the spectral phase consists simply of measuring $\Delta S_{\mathrm{pr}}(\omega)$ versus pump–probe delay τ_p and identifying the location of the central minimum ω_0, which is well reproduced by the analytical model described in the previous section. As long as $\phi_s'(\omega)$ is monotonic, $\phi'(\omega_0) = \tau_p(\omega_0)$ is single-valued. This can be ensured over a given frequency interval for large enough β_2 with respect to higher-order coefficients β_n. This equation is then directly integrated to find $\phi_s(\omega)$ or fit to $\sum c_n(\omega - \omega_c)^n$ to yield the dispersion coefficients $\beta_n = (n!)^{-1}(\partial^n\phi/\partial\omega^n)_{\omega_c} = nc_{n-1}$ for $n \geq 2$. One way to understand how the technique works is described as follows: Transient phase perturbation of the probe produces frequency components over some bandwidth determined by the duration of the phase perturbation. These components interfere with the unperturbed probe components to produce spectral amplitude oscillations. By measuring their dependence on the probe time delay, we can find the group delay across the probe spectrum. This technique is similar to well-known techniques often employed for characterizing compressors and stretchers [11,12] and a recently developed technique that uses sum frequency generation between a chirped pulse and a short pulse [13].

As an aside, we note that the SC spectral phase also could be determined using pulse characterization techniques such as SPIDER [14] or FROG [15]. However, each of these methods requires a dedicated and complex apparatus, which can be challenging to implement for highly chirped, wide-bandwidth pulses. In addition, these techniques require the pulse to propagate through air, lenses, and beam splitters before measurement, leading to potential systematic errors.

We next demonstrate the technique in experiments. The experimental setup is the same as described in [3]. The probe/reference SC is generated by filamentation of a 40 fs, ~200 μJ pulse in a gas cell filled with 2.7 atm Xe. The probe/reference beam is combined with the pump beam using a dichroic mirror and focused on a thin gas target [2] inside a vacuum chamber. The pump beam was focused at $f/30$ and the probe/reference beam at $f/150$. Example data, using Ar with a 50 fs pulse at a peak intensity of ~60 TW/cm^2, below the appearance of ionization [2], is shown in Fig. 3. Figure 3(a) shows the probe spectra with ($|E_{\mathrm{pr}}(\omega)|^2$, solid black line) and without ($|\overline{E}_{\mathrm{pr}}(\omega)|^2$, dashed red line) the pump present, for a pump–probe time delay we define as $\tau_p = 0$, for which the pump pulse overlaps with $\omega_0 = 3.28$ fs^{-1}. The differential probe spectrum $\Delta S_{\mathrm{pr}}(\omega)$ is shown in Fig. 3(b) for $\tau_p = -1$, 0, and 1 ps. A map of $\Delta S_{\mathrm{pr}}(\omega)$ captured as a function of pump–probe delay τ_p, in steps of 13.3 fs, scanned by a computer-controlled stage, is shown in Fig. 3(c), with the location of the central minimum following $\tau_p(\omega_0) = \phi'(\omega_0)$. At each delay, $\Delta S_{\mathrm{pr}}(\omega)$ is formed as a multishot average of 40 difference spectra. Note that if the spectral phase was purely quadratic, the dependence would be linear. The curvature observed indicates higher-order dispersion.

We find that the minimum order typically required to achieve a good polynomial fit is third-order; from this data set, we find $\beta_2 = 1956$ fs^2, $\beta_3 = 386$ fs^3, and $\beta_4 = 168$ fs^4. The residual of the fit is shown in Fig. 3(d) for a third-order polynomial (dashed red) and a fourth-order polynomial

(solid black). Note that the technique is not restricted to a polynomial spectral phase model [Eq. (4)]. Even with the fourth-order polynomial fit, there are residual oscillations with an amplitude of ~0.2 rad. These oscillations can be neglected or included in the extraction procedure. All that is required for the measurement technique to work is a one-to-one relationship between the pump–probe time delay and the probe frequency within the frequency interval of interest. This depends on the magnitude of β_2 with respect to higher-order spectral phase coefficients.

As described, the procedure for determining the probe spectral phase involves a multishot delay scan, so it is crucial in SSSI experiments to have a certain amount of shot-to-shot spectral phase stability. A single-shot measurement of $\Delta S_{\mathrm{pr}}(\omega)$ carries information on the spectral phase of a region $\Delta\omega$ of the probe spectrum of order the pump pulse bandwidth, and this can be used to test the local phase stability. The spectral locations of the extrema of the oscillations in $\Delta S_{\mathrm{pr}}(\omega)$ depend on $\phi_s(\omega)$, as is clear in Eq. (5). The differential probe spectrum is shown for 40 consecutive shots in Fig. 4(a). If $\phi_s(\omega)$ were unstable, one would see the position of the oscillations shift from shot to shot. Instead, we observe a very stable pattern. We can more precisely assess this stability using Eq. (5), where the extrema occur at ω satisfying $n\pi = \phi_s(\omega) - \phi_s(\omega_0) + (\omega - \omega_0)\tau_p + \pi/4$, where n is an integer. Thus, for each shot, we can find the values of $\phi_s(\omega)$ at the spectral locations of the extrema, as plotted in Fig. 4(b), along with a second-order polynomial fit.

The extracted values of β_2 from each shot, shown in Fig. 4(c), are scattered (likely because of increased noise in the single-shot spectra) but close to the above value of $\beta_2 = 1956$ fs^2 extracted from the wider spectrum fit to the averaged, multishot curve of Fig. 3(c). We attribute the lower average value of β_2 observed in Fig. 4(c) to inaccuracy of the stationary phase approximation model for $\Delta S_{\mathrm{pr}}(\omega)$ [Eq. (5)]. It should be noted that, for noise reduction, multiple interferograms are typically averaged together before phase extraction [16], so accurate extraction requires knowledge of the *average* spectral phase, which is exactly what the multishot technique described here measures.

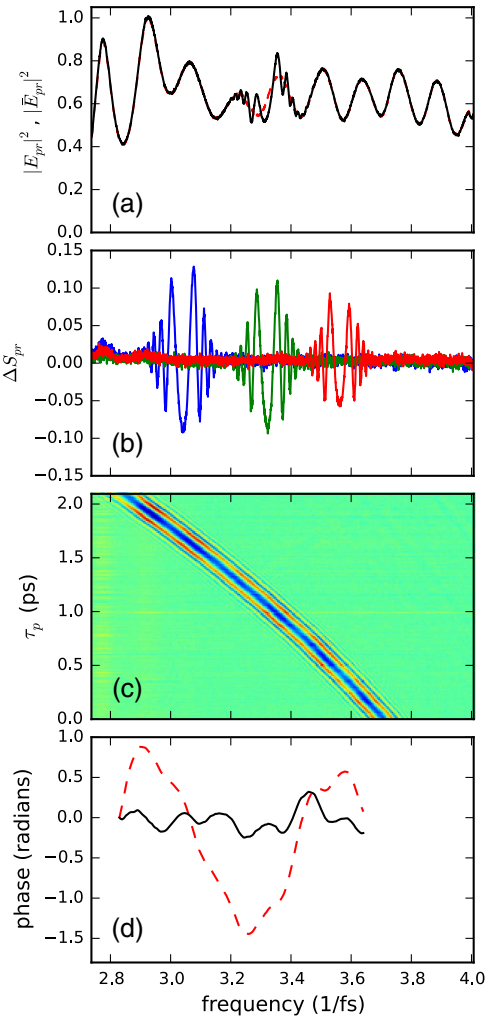

Fig. 3. Extraction of the spectral phase in Ar. (a) Example SC spectra with the pump pulse present (solid black) and absent (dashed red). (b) Differential probe spectrum for $\tau_p = -1$, 0, and 1 ps. (c) Differential probe spectrum as a function of pump–probe delay τ_p. (d) Integrated residuals of a second-order (dashed red) and third-order (solid black) polynomial fit of $\phi_s'(\tau_p)$, corresponding to the third- and fourth-order polynomial fits to $\phi_s(\tau_p)$.

5. LIMITS ON SSSI TIME RESOLUTION

A. Limits Imposed By Accuracy of Spectral Phase Determination

An important source of distortion in the extracted time domain phase is uncertainty in the probe spectral phase measurement. Distortion appears in the extracted temporal phase when the spectral phase error within the affected part of the probe spectrum approaches 1 radian. The width $\Delta\omega_t$ of the affected probe spectrum is inversely proportional to the duration τ_w of the pump-induced probe transient, $\Delta\omega_t \approx 4\pi/\tau_w$. This can be used in Eq. (4) to find the maximum allowable error in the spectral phase coefficients. To avoid distortion, the error in the nth coefficient must satisfy $\Delta\beta_n < [\tau_w/\pi]^n$. As an example, for a transient 10 fs long, the error in $\beta_2(\beta_3)$ must be less than 10 fs^2(32 fs^3). The shorter the phase transient, the greater the required precision. This illustrates the need for precise characterization of the probe spectral phase.

As a demonstration of the effect of error in the probe spectral phase, Fig. 5 shows simulated time-domain phase traces for a 10 fs phase perturbation, where the probe spectral phase is given by Eq. (4), with spectral phase coefficients $\beta_2 = 500$ fs^2 and $\beta_3 = 100$ fs^3. The top (black) curve shows the actual phase shift. The blue curve shows the phase shift extracted using the correct coefficients. The green curve shows the phase shift extracted neglecting β_3. The red curve shows the phase shift extracted using a value of β_2 5% larger.

B. Limits Imposed By Spectral Resolution

Another important and previously unrecognized practical constraint concerns the spectral resolution of the phase extraction. The issue can be understood by examining Figs. 1 and 2. In order to reconstruct the refractive index perturbation in the time domain, one must be able to resolve the pump-induced spectral oscillations in the spectral amplitude. As can be seen,

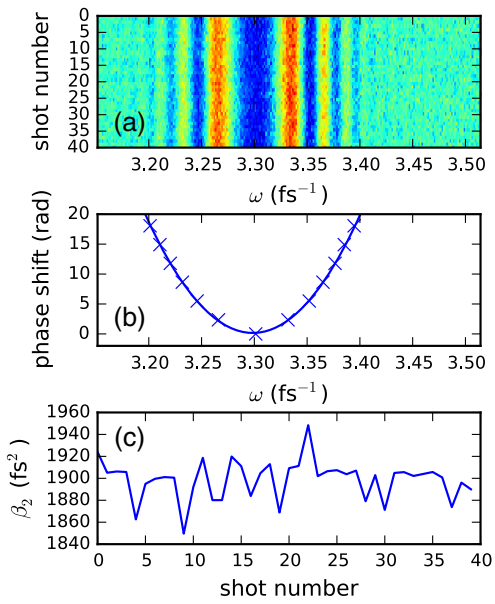

Fig. 4. Testing the local phase stability by analyzing single-shot differential probe spectra. (a) Differential probe spectrum for 40 consecutive laser shots. (b) Spectral locations of extrema for one shot, and a polynomial fit. (c) The second-order phase parameter β_2 found from the fit as a function of shot.

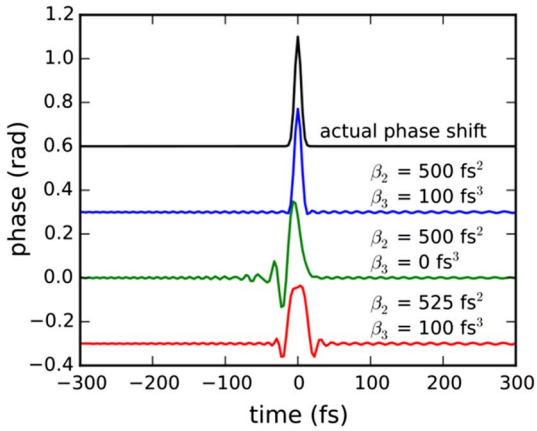

Fig. 5. Simulated effect of uncertainty in the probe spectral phase. Top black curve shows the actual 10 fs pump-induced phase transient. Bottom three curves show, from top to bottom, the phase shift extracted assuming the correct probe dispersion parameters, neglecting third-order dispersion, and using a second-order dispersion parameter that is 5% too large.

the oscillations become more rapid as $|\omega - \omega_0|$ increases. This is because the oscillations are primarily due to the cosine factor in Eqs. (5) and (6), the argument of which is, to the lowest order, quadratic in $\omega - \omega_0$ because of the β_2 term. Neglecting β_n for $n > 2$, the spectral period of the pump-induced oscillations is approximated by $\Delta\omega_{\text{osc}} \approx \pi/|\beta_2(\omega - \omega_0)|$. The shortest measurable pump-induced probe transient produces modulations covering the entire SC bandwidth $\Delta\omega$. In this case, $\Delta\omega_{\text{osc}}^{\text{min}} \approx 2\pi/|\beta_2\Delta\omega|$ is the minimum spectral modulation period produced (located on the edges of the SC spectrum). Thus, to achieve the ultimate time resolution of SSSI, we require sufficient spectral resolution in the phase and amplitude extracted from the interferogram to resolve these oscillations.

The spectral resolution of spectral interferometry depends on the probe/reference time delay τ_r. The period of the probe/reference interference fringes is $2\pi/\tau_r$. Assuming the interference fringes are well resolved [17], the best achievable spectral resolution in the extracted spectral phase and amplitude is set by the Nyquist criterion to be twice the fringe spacing or $\Delta\omega_s^{\text{min}} = 4\pi/\tau_r$. Note that the imaging spectrometer's resolution determines the maximum achievable τ_r and, thus, sets $\Delta\omega_s^{\text{min}}$. The requirement that $\Delta\omega_s^{\text{min}} < \Delta\omega_{\text{osc}}^{\text{min}}$ can be used to derive a necessary condition for achieving the ultimate time resolution:

$$|\beta_2\Delta\omega| < \frac{\tau_r}{2}. \tag{7}$$

The length of the chirped probe pulse is approximately $2|\beta_2\Delta\omega|$; thus, Eq. (7) implies that the duration of the probe and reference pulses must be less than the time delay between the probe and reference pulses. Using $\Delta\omega \approx 2\pi/\tau_w$ for a phase transient of FWHM duration τ_w, an alternative condition is

$$|\beta_2\tau_r^{-1}| < \frac{\tau_w}{4\pi}. \tag{8}$$

The consequence of not satisfying Eq. (8) is illustrated in Fig. 6. Figure 6(a) shows the frequency domain amplitude

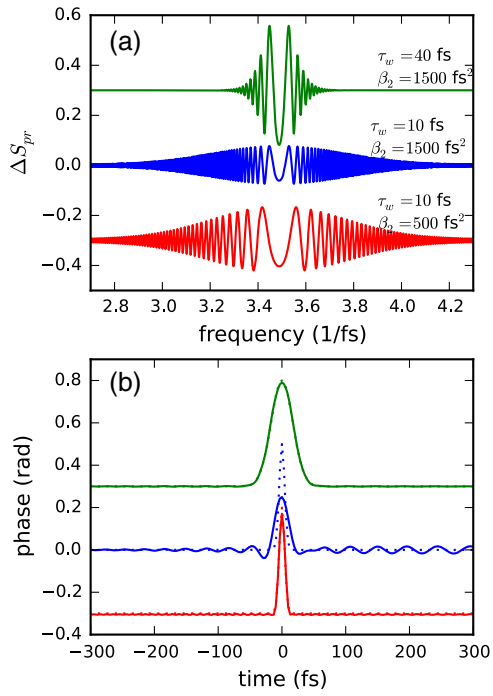

Fig. 6. Illustration of the effect of insufficient spectral resolution in the phase extraction. (a) Probe amplitude change $\Delta S_{\text{pr}}(\omega)$ for a 40 fs pump pulse and a probe pulse with $\beta_2 = 1500$ fs^2 (top), for a 10 fs pump pulse and a probe pulse with $\beta_2 = 1500$ fs^2 (middle), and for a 10 fs pump pulse and a probe pulse with $\beta_2 = 500$ fs^2 (bottom). (b) Simulated extraction (solid lines) of time domain phase shift for the three cases in (a), assuming a probe/reference time delay of $\tau_r = 1$ ps. Dotted lines show the actual time-domain phase shift.

change for a Gaussian phase perturbation of duration $\tau_w = 40$ fs (top trace) and $\tau_w = 10$ fs (middle and bottom traces), and a probe pulse with $\beta_2 = 1500$ fs^2 (top and middle traces) and $\beta_2 = 500$ fs^2 (bottom trace). Figure 6(b) shows the extracted time domain phase shift corresponding to the traces in Fig. 6(a), using $\tau_r = 1$ ps. When β_2/τ_r is too large, as is the case for the middle trace, oscillations appear before and after the main pulse, and the peak phase shift is reduced. An optimized SSSI setup should have as little glass as possible in the path after the generation of supercontinuum to minimize β_2, while maintaining enough chirp so that the transient of interest is covered by the probe pulse of duration $2\beta_2\Delta\omega$. Note that minimizing the length of glass in the supercontinuum path also has the effect of minimizing higher-order spectral phase coefficients. Thus, monotonicity of $\phi_s'(\omega)$, a requirement of the spectral phase measurement technique presented in Section 4, is easily satisfied in practice. The spectrometer resolution also should be optimized so that the probe/reference time delay τ_r can be maximized.

6. CONCLUSIONS

In summary, we have discussed how to optimize SSSI to achieve its ultimate time resolution given by the inverse probe bandwidth. Using a simple analytical model, we illustrated the effect of a small, transient phase perturbation on a chirped probe pulse. We described a simple *in situ* technique for measuring to arbitrary-order the spectral phase of chirped, broadband probe pulses. Then, we illustrated the need for precise measurement of the probe spectral phase for extraction of short phase transients. Finally, we derived a relationship between the magnitude of the probe chirp, the time delay between the probe and reference pulses, and the shortest resolvable phase transient.

Funding. National Science Foundation (NSF) (PHY1301948); U.S. Department of Energy (DOE) (DESC0007970); Air Force Office of Scientific Research (AFOSR) (FA95501310044); Army Research Office (ARO) (W911NF1410372).

Acknowledgment. We thank J. A. Elle for technical assistance, and we acknowledge B. Miao and A. J. Goers for discussions.

REFERENCES

1. K. Y. Kim, I. Alexeev, and H. M. Milchberg, "Single-shot supercontinuum spectral interferometry," Appl. Phys. Lett. **81**, 4124–4126 (2002).
2. J. K. Wahlstrand, Y.-H. Cheng, Y.-H. Chen, and H. M. Milchberg, "Optical nonlinearity in Ar and N_2 near the ionization threshold," Phys. Rev. Lett. **107**, 103901 (2011).
3. J. K. Wahlstrand, Y.-H. Cheng, and H. M. Milchberg, "High field optical nonlinearity and the Kramers–Kronig relations," Phys. Rev. Lett. **109**, 113904 (2012).
4. J. K. Wahlstrand, Y.-H. Cheng, and H. M. Milchberg, "Absolute measurement of the transient optical nonlinearity in N_2, O_2, N_2O, and Ar," Phys. Rev. A **85**, 043820 (2012).
5. Y.-H. Chen, S. Varma, A. York, and H. M. Milchberg, "Single-shot, space- and time-resolved measurement of rotational wavepacket revivals in H_2, D_2, N_2, O_2, and N_2O," Opt. Express **15**, 11341–11357 (2007).
6. J. K. Wahlstrand, S. Zahedpour, Y.-H. Cheng, J. P. Palastro, and H. M. Milchberg, "Absolute measurement of the ultrafast nonlinear electronic and rovibrational response in H_2 and D_2," Phys. Rev. A **92**, 063828 (2015).
7. S. Zahedpour, J. K. Wahlstrand, and H. M. Milchberg, "Measurement of the nonlinear refractive index of air constituents at mid-infrared wavelengths," Opt. Lett. **40**, 5794–5797 (2015).
8. L. Lepetit, G. Chériaux, and M. Joffre, "Linear techniques of phase measurement by femtosecond spectral interferometry for applications in spectroscopy," J. Opt. Soc. Am. B **12**, 2467–2474 (1995).
9. M. Takeda, H. Ina, and S. Kobayashi, "Fourier-transform method of fringe-pattern analysis for computer-based topography and interferometry," J. Opt. Soc. Am. **72**, 156–160 (1982).
10. E. Tokunaga, A. Terasaki, and T. Kobayashi, "Induced phase modulation of chirped continuum pulses studied with a femtosecond frequency-domain interferometer," Opt. Lett. **18**, 370–372 (1993).
11. J. Piasecki, B. Colombeau, M. Vampouille, C. Froehly, and J. A. Arnaud, "Nouvelle méthode de mesure de la réponse impulsionnelle des fibres optiques," Appl. Opt. **19**, 3749–3755 (1980).
12. C. Sáinz, P. Jourdian, R. Escalona, and J. Calatroni, "Real time interferometric measurements of dispersion curves," Opt. Commun. **111**, 632–641 (1994).
13. A. Zeytunyan, A. Muradyan, G. Yesayan, L. Mouradian, F. Louradour, and A. Barthélémy, "Generation of broadband similaritons for complete characterization of femtosecond pulses," Opt. Commun. **284**, 3742–3747 (2011).
14. G. Stibenz and G. Steinmeyer, "High dynamic range characterization of ultrabroadband white-light continuum pulses," Opt. Express **12**, 6319–6325 (2004).
15. T. C. Wong, M. Rhodes, and R. Trebino, "Single-shot measurement of the complete temporal intensity and phase of supercontinuum," Optica **1**, 119–124 (2014).
16. Y.-H. Chen, S. Varma, I. Alexeev, and H. M. Milchberg, "Measurement of transient nonlinear refractive index in gases using xenon supercontinuum single-shot spectral interferometry," Opt. Express **15**, 7458–7467 (2007).
17. C. Dorrer, N. Belabas, J. P. Likforman, and M. Joffre, "Spectral resolution and sampling issues in Fourier-transform spectral interferometry," J. Opt. Soc. Am. B **17**, 1795–1802 (2000).